# GCEE

*by* Gcee Gcee

**Submission date:** 28-Aug-2023 10:57AM (UTC+0700)
**Submission ID:** 2152496673
**File name:** GCEE_UHPC_R.0_Albert_Antoni.docx (141.3K)
**Word count:** 2976
**Character count:** 17164

# Mechanical Activation of OPC for Lower Strength UHPC with Reduced Silica Fume Content

Albert Kuncoro[1, a)], Antoni Antoni[1, b)], Juan Felix Indrianto[1, c)], Jonathan Rayhan[1, d)], Tri Eddy Susanto[2, e)] and Djwantoro Hardjito[1, f)]

[1]*Department of Civil Engineering, Petra Christian University*
*Jl. Siwalankerto No. 121-131, Siwalankerto, Kec. Wonocolo, Surabaya, Jawa Timur, Indonesia 60236*
[2]*Research & Development of PT Semen Indonesia (Persero) Tbk.*
*Jl. Veteran No.93, Kec. Gresik, Kab. Gresik, Jawa Timur, Indonesia 61122*

[a)]albertk@petra.ac.id
[b)]Corresponding author: antoni@petra.ac.id
[c)]juanfelixindrianto@gmail.com
[d)]jonathan.rayhan@yahoo.com
[e)]tri.susanto@sig.id
[f)]djwantoro.h@petra.ac.id

**Abstract.** Ultra-High-Performance Concrete (UHPC) traditionally exhibits compressive strength exceeding 150 MPa. However, variants have been identified with slightly lesser strengths that still surpass those of standard concrete; these are termed Lower Strength Ultra-High-Performance Concrete (LSUHPC). This study focused on the strategic utilization of Ordinary Portland Cement (OPC) in LSUHPC formulation while significantly curtailing the extensive use of silica fume, which is a common practice in UHPC production. Typically, high-performance concrete, with strengths ranging from 120-150 MPa, is produced using fine aggregates, heavy doses of silica fume, superplasticizer, and fiber. Contrary to this traditional method, our research developed an LSUHPC mix design with a significantly reduced volume of silica fume. For the current research stage, the use of steel fiber was omitted. To counteract the reduction in silica fume, the OPC was subjected to mechanical grinding to enhance its particle fineness and reactivity. Additionally, a low volume of class F fly ash was incorporated into the mixture to improve its workability. This adjustment was theorized to diminish inter-particle voids, reduce the water requirement, and increase the mixture's density. With a fixed superplasticizer dosage of 4%, the aim was to minimize the water-to-binder ratio, maintaining workability and achieving enhanced particle packing and compressive strength. Following a series of grinding, particle fineness analysis, mix design formulations, and consistency tests, it was confirmed that the strategic application of OPC, combined with fly ash and reduced silica fume levels in the LSUHPC formulation, can achieve the targeted high compressive strength. This approach opens the door for cost-efficient LSUHPC production by drastically reducing the use of silica fume.

## INTRODUCTION

Concrete is the most used construction material in the world. As time progresses, numerous new innovations have been developed in response to the diverse needs and demands within the construction industry. The advancement of the construction sector increases the need for higher-quality concrete, especially in the construction of large-scale structures such as bridges, high-rise buildings, flyovers, and dams, which require concrete structures with exceptional performance. Consequently, it is vital to develop concrete with high quality that can effectively address market demands as a viable solution [1]. UHPC is concrete with a compressive strength greater than or

equal to 150 MPa. UHPC with strength ranging from 130-150 MPa is referred to as the Lower Strength UHPC (LSUHPC)[2], [3].

There are four main factors that determine the strength of UHPC: reduced porosity, advancements in microstructure, increased homogeneity, and enhanced density. UHPC can be produced with a low water-to-binder ratio by eliminating coarse aggregates, incorporating steel fibers, adding superplasticizer, and utilizing supplementary cementitious materials (SCMs) such as fly ash, silica fume, and ground granulated blast-furnace slag[4]. On the other hand, the lower bound UHPC can be made using the same materials as conventional UHPC, with or without fiber additions. However, the use of materials like silica fume, steel fiber, and superplasticizer significantly escalates the cost of UHPC. This issue can be mitigated by partially substituting the binder by adding cheap and widely available SCMs, creating a denser matrix, thereby reducing the demand for superplasticizers and silica fume [5]–[7]. In numerous studies on UHPC, the optimal dosage of silica fume as SCMs to achieve the desired strength typically ranges between 15-20% of the total binder weight [8], [9]. Despite its exceptional performance as SCMs, silica fume has a drawback, it costs about 25 times more than conventional cement. Additionally, due to its high incorporation rate, the specific surface area (SSA) of the fines increases, demanding higher water requirements or increased superplasticizer dosage. These factors contribute significantly to the high production cost of UHPC.

Mechanical activation of cement involves milling cement particles, which allows them to be broken down into finer particles, which can enhance reactivity and fill small voids within the concrete. The outcomes of mechanical activation are significantly influenced by the method and duration of processing [10]. By mechanically activating the cement particles and properly grading the fines, resulting in reduced silica fume usage, the concrete density could be substantially increased. Optimal density can effectively exert water from the concrete matrix, leading to reduced water needs and a subsequent decrease in superplasticizer usage [11]–[13]. The heightened density and reduced water used in concrete could enhance concrete performance in both fresh and hardened states [14].

This paper presents the potential for developing cost-effective LSUHPC by minimizing silica fume use and excluding steel fiber addition. This outcome was achieved through the mechanical activation of cement and grading fine particles, enhancing concrete density, and altering the milling duration. Additionally, properties of the raw materials, mechanical attributes of the LSUHPC, and a microstructural analysis are discussed.

## MATERIALS AND METHOD

### Mix Proportion of Materials

The binder proportions for the three control mortar mixtures and for the fourteen experimental mortar mixtures are presented in TABLE 1 and TABLE 2, respectively. This experimental study encompassed four variations of OPC and class F fly ash (FFA) blend proportions, three variations in silica fume content, and combinations of 8-hour and 16-hour milled-OPC. For all mix designs, the sand-to-binder ratio was consistently maintained at 1:1.5 by mass. The superplasticizer addition was fixed at 4% of the total binder content across all mix designs. The water-to-binder ratio (w/b) was adjusted to achieve a target flow diameter value of 15±1cm, as determined by the flow table test, and the specific values were subsequently recorded.

### Sample Preparation

In this study, specimens were prepared as 50-mm cubes to analyze their mechanical behavior. The material preparation and mortar casting were undertaken through several sequential procedures. Initially, data regarding the raw materials were collected and analyzed, including evaluations of specific gravity, normal consistency, particle size analysis (PSA), and chemical composition. The grinding of OPC was facilitated using a ball mill machine with dimensions of 35 cm in diameter and 41 cm in length. This machine operated at 60 rotations per minute and utilized 30mm cylpebs as grinding media. The set cylpebs-to-material ratio during this grinding phase was 5:1, and each grinding session produced 5 kg of finely ground material.

After the preparation of the binder, the control mortar specimens were cast, followed closely by the casting of the experimental mortar specimens. During the mixing phase, the dry powder constituents were blended first. This was followed by a gradual addition of water and superplasticizer. It's noteworthy that the superplasticizer was added in two stages; initially, 2% was incorporated, with the remaining quantity added just prior to the flow table test. Water additions were adjusted to meet the target flow diameter. As soon as the mixture achieved this desired flow diameter, the necessary water volume was recorded, setting the stage for mortar casting.

The compaction and casting of the specimens followed the ASTM C109/109M standards. Once the casting process was finalized, the specimens were secured with plastic cling wrap. A day post-casting, they were extracted from their molds and then transitioned into a water immersion regime for curing. This curing process continued until the specimens reached a predefined age, marking them ready for subsequent testing.

**TABLE 1.** Binder Proportions by Mass of Control Mortar Specimens

| Code | Binder (%) | |
|---|---|---|
| | Blend of 70% OPC + 30% FFA | Silica Fume (SF) |
| MC-SF0 | 100% | 0% |
| MC-SF5 | 95% | 5% |
| MC-SF10 | 90% | 10% |

**TABLE 2.** Binder Proportions by Mass of Mortar Specimens

| Code | Binder (%) | | | |
|---|---|---|---|---|
| | 70% OPC + 30% FFA (CF) | Silica fume (SF) | 8-h Milled OPC (E) | 16-h Milled OPC (S) |
| CF75-SF0-E25 | 75% | 0 | 25% | 0 |
| CF75-SF0-E18.75-S6.25 | 75% | 0 | 18.75% | 6.25% |
| CF75-SF2.5-E16.8-S5.7 | 75% | 2.5% | 16.80% | 5.70% |
| CF75-SF2.5-E7.5-S2.5 | 75% | 2.5% | 15.00% | 7.50% |
| CF75-SF5-E15-S5 | 75% | 5% | 15% | 5% |
| CF75-SF5-E5-S15 | 75% | 5% | 5% | 15% |
| CF65-SF5-E20-S10 | 65% | 5% | 20% | 10% |
| CF65-SF5-E10-S20 | 65% | 5% | 10% | 20% |
| CF60-SF5-E25-S10 | 60% | 5% | 25% | 10% |
| CF60-SF5-E10-S25 | 60% | 5% | 10% | 25% |
| CF50-SF5-E30-S15 | 50% | 5% | 30% | 15% |
| CF50-SF5-E15-S30 | 50% | 5% | 15% | 30% |
| CF40-SF5-E35-S20 | 40% | 5% | 35% | 20% |
| CF40-SF5-E20-S35 | 40% | 5% | 20% | 35% |

## Sample Testing

Tests on the raw materials encompassed chemical composition assessment using X-ray fluorescence (XRF), particle size analysis (PSA), normal consistency in accordance with ASTM C187, specific gravity as per ASTM C188, and peak hydration temperature (or reactivity) testing. The PSA was executed at the Analysis and Measurement Service Laboratory within the FMIPA Chemistry Department of Brawijaya University, Malang. Notably, the X-ray fluorescence test, aligned with ASTM D4326 standards, was conducted at PT Sucofindo Analytical and Testing Laboratories in Surabaya, employing a CILAS type 1090 instrument for the PSA.

Regarding the tests on the fresh state of the mortar, the flow table test was done based on ASTM C230. The resultant flow from this test provided a key reference point to determine the water requirement, which is then expressed as the water-to-binder (w/b) ratio. The test for hardened mortar included compressive strength testing, following the ASTM C109, alongside density and ultrasonic pulse velocity (UPV) tests.

# RESULTS AND DISCUSSION

## Raw Material Properties

The results of the XRF testing are presented in TABLE 3. According to ASTM C618 [15], the analyzed fly ash sample is classified as class F fly ash. In this study, the most dominant chemical compound in the fly ash material is

$SiO_2$, with a volume percentage of 44.09. This is followed by $Al_2O_3$, $Fe_2O_3$, and CaO, which have values of 17.5, 15.57, and 10.71, respectively.

The results of the PSA testing between OPC and class F fly ash (FFA) materials can be observed in FIGURE 1. The PSA results indicate that the size of the OPC sample is smaller compared to FFA, as evidenced by the OPC curve being positioned to the left side of the FFA curve on the graph, indicating a smaller-sized particle which is uncommon. The result was probably due to the OPC obtained from the ready-mix silo dust filter, and further examination is needed to confirm the particle size distribution of the untreated OPC.

**TABLE 3.** Chemical Composition of Class-F Fly Ash

| Chemical Composition | Percentage (%) |
|---|---|
| $SiO_2$ | 44.09 |
| $Al_2O_3$ | 17.5 |
| $Fe_2O_3$ | 15.57 |
| CaO | 10.71 |
| MgO | 6.16 |
| $Na_2O$ | 1.66 |
| $K_2O$ | 0.94 |
| $TiO_2$ | 0.79 |
| $MnO_2$ | 0.29 |
| $P_2O_5$ | 0.24 |
| $SO_3$ | 1.59 |

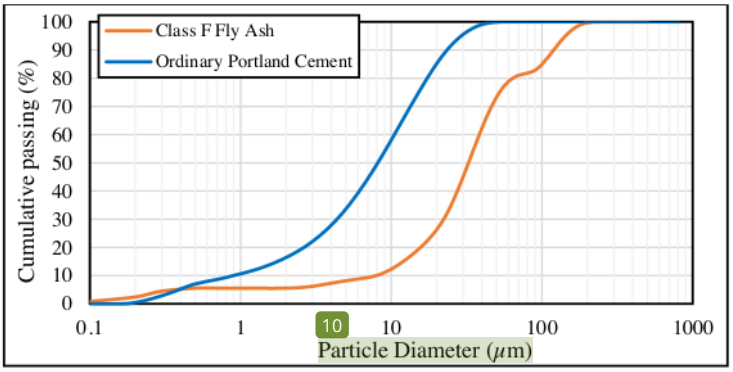


**FIGURE 1.** Particle Size Analysis (PSA) of OPC and FFA

## Grinding Performance

FIGURE 2 and TABLE 4 display the PSA results for untreated OPC, 8-hours milled OPC, and 16-hours milled OPC samples. As the duration of grinding extends, there is a notable reduction in the particle size of the OPC, indicating increased fineness. This heightened fineness concurrently improves reactivity, normal consistency, and specific gravity, as illustrated in Figure 3. A surge in fineness subsequently leads to an augmented specific surface area, which in turn results in a rise in normal consistency and reactivity due to the increase in free-CaO [16].

**TABLE 4.** PSA Result of untreated OPC, 6-hours, and 8-hours Milled OPC

| Binder | Median (μm) | Mean (μm) | Modus (μm) |
|---|---|---|---|
| Ordinary Portland Cement (OPC) | 7.955 | 6.145 | 10.756 |
| 8 Hours – Milled OPC | 6.013 | 5.12 | 6.75 |
| 16 Hours – Milled OPC | 4.018 | 3.417 | 5.348 |

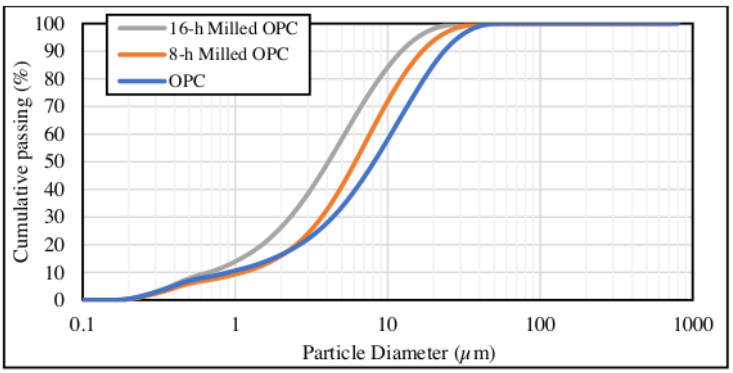


**FIGURE 2.** PSA of OPC, 6-hours, and 8-hours Milled OPC

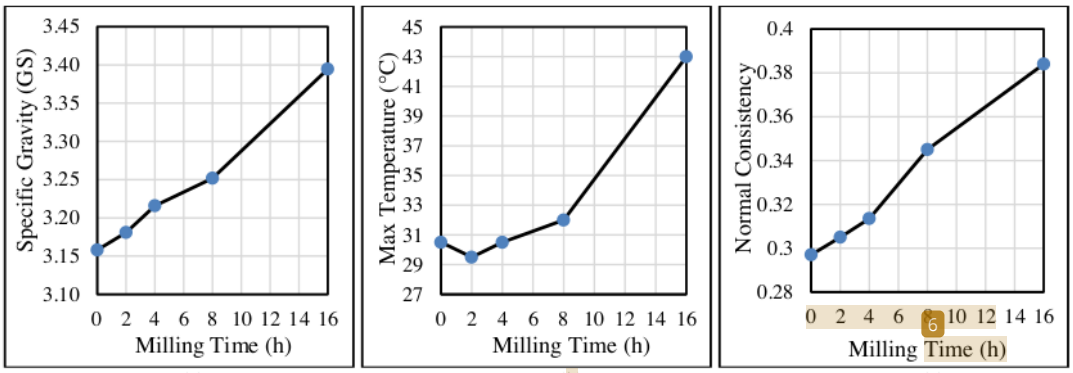


(a) (b) (c)

**FIGURE 3.** Properties of Milled OPC: (a). Specific Gravity, (b). Temperature of Reaction, (c). Normal Consistency

## Compressive Strength Performance

**FIGURE *4*** presents the results and analysis of both compressive strength and w/b. Notably, the specimen labeled CF50-SF5-E15-S30 exhibits the highest compressive strength, registering at 134.48 MPa. This surpasses the compressive strength of the control mortar specimen MC-SF10 (which has an added 10% silica fume), coming in at 124.82 MPa. This superior performance of the CF50-SF5-E15-S30 specimen can be attributed to its denser constitution in comparison to the MC-SF10 control, with density values standing at 2.39 and 2.34 respectively. These findings highlight that the objective of achieving high density isn't solely reliant on the incorporation of super-fine materials. Preserving an optimal gradation at the microstructural level plays a pivotal role in augmenting the material's performance. Moreover, as illustrated in **FIGURE *4***, the w/b ratios for the specimens can be decreased to a significant low of 0.19, underscoring its potential to bolster the overall mechanical performance of the concrete.

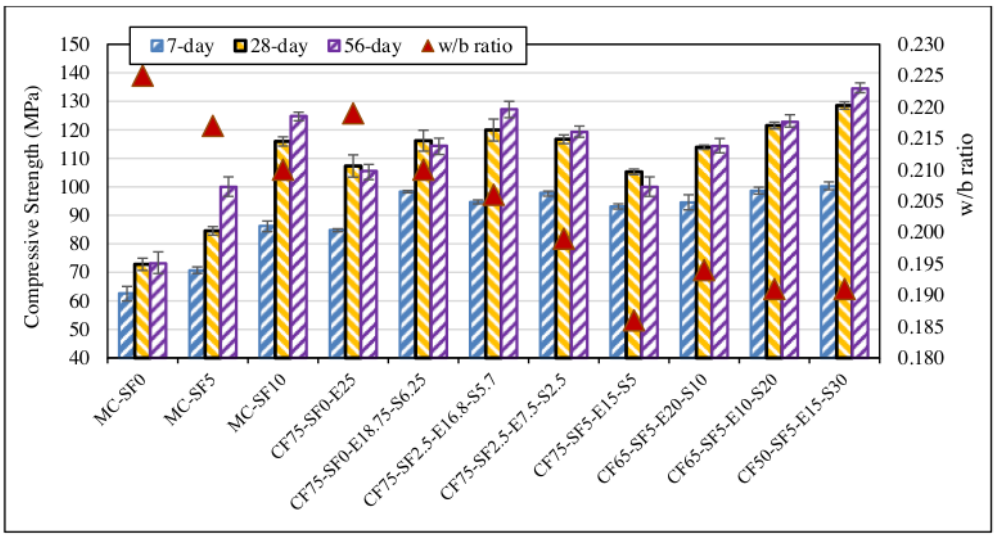


**FIGURE 4.** Relationship between Compressive Strength and w/b Ratio on Various Specimens.

## Density

As depicted in FIGURE 5, an increase in density correlates with higher UPV values. This correlation can be attributed to the fact that denser materials facilitate a more efficient propagation of ultrasonic waves within their solid structure. Ultrasonic waves travel more effectively through solid media compared to air. In the context of concrete's mechanical performance, this implies a more evenly distributed force, enabling the material to support greater loads [17].

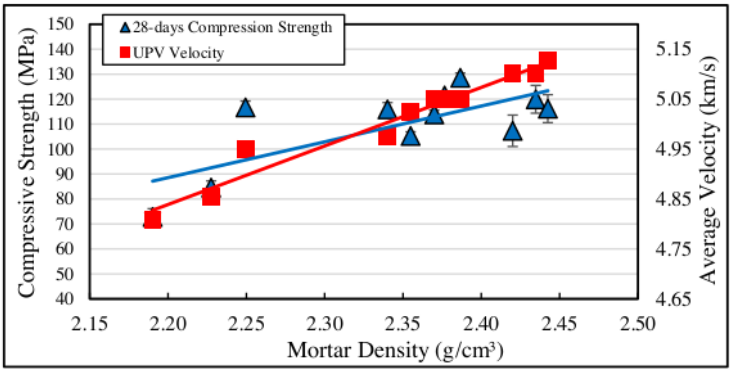


**FIGURE 5.** Relationship between Compressive Strength and UPV Velocity on Various Degree of Mortar's Density.

## CONCLUSION

The results of this research confirm that Lower Strength Ultra-High-Performance Concrete (LSUHPC) can be produced cost-effectively by reducing the usage of pricier materials. When incorporating silica fume into LSUHPC, a careful adjustment through a systematic microstructural particle gradation is essential to achieve the desired density. The findings highlight that the specimen labeled CF50-SF5-E15-S30 achieved the highest compressive strength at 134.48 MPa, outperforming the control mortar specimen MC-SF10, which recorded a strength of 124.82

MPa at 56 days. This superior performance of the CF50-SF5-E15-S30 specimen can be attributed to its increased density compared to the MC-SF10 control. This denser nature allowed for a reduction in the water-to-binder (w/b) ratio in CF50-SF5-E15-S30 to an impressive low of 0.19. Additionally, the meticulous grinding of OPC notably heightened its reactivity. The PSA results emphasize the importance of grinding in achieving desired concrete properties. This enhanced reactivity is evident in the improved compressive strength of the CF75-SF2.5-E16.8-S5.7 sample, which exceeded the MC-SF10 control mortar by 12 MPa after a mere 7 days of curing. Furthermore, the direct correlation between density and UPV indicates a uniformly structured LSUHPC that can efficiently distribute forces. This research also brings forth economic implications by advocating for a more cost-effective construction approach without quality compromise and suggests potential avenues for further optimization in LSUHPC production.

## ACKNOWLEDGMENTS

We extend our heartfelt appreciation for the collaborative research opportunity made possible by the Memorandum of Understanding (MOU) between Petra Christian University and PT Semen Indonesia (persero) Tbk. This collaboration has profoundly enriched and broadened the horizons of our research."

## REFERENCES

1. F. Sciarretta *et al*., "Ultra-High performance concrete (UHPC) with polypropylene (Pp) and steel Fibres: Investigation on the high temperature behaviour," *Constr Build Mater*, vol. 304, p. 124608, Oct. 2021, doi: 10.1016/j.conbuildmat.2021.124608.
2. A. Kuncoro, H. D. Pranoto, L. W. Sacca, A. Antoni, D. Hardjito, and E. Tanojo, "Evaluation of bonding performance of ultra high-performance concrete with fly ash content as overlay on normal strength concrete.," *IOP Conf Ser Earth Environ Sci*, vol. 1195, no. 1, p. 012020, Jun. 2023, doi: 10.1088/1755-1315/1195/1/012020.
3. N. M. Azmee and N. Shafiq, "Ultra-high performance concrete: From fundamental to applications," *Case Studies in Construction Materials*, vol. 9, p. e00197, Dec. 2018, doi: 10.1016/j.cscm.2018.e00197.
4. C. Shi, Z. Wu, J. Xiao, D. Wang, Z. Huang, and Z. Fang, "A review on ultra high performance concrete: Part I. Raw materials and mixture design," *Constr Build Mater*, vol. 101, pp. 741–751, Dec. 2015, doi: 10.1016/j.conbuildmat.2015.10.088.
5. A. K. Akhnoukh and C. Buckhalter, "Ultra-high-performance concrete: Constituents, mechanical properties, applications and current challenges," *Case Studies in Construction Materials*, vol. 15, p. e00559, Dec. 2021, doi: 10.1016/j.cscm.2021.e00559.
6. A. Kuncoro and H. S. Djayaprabha, "The Effect of Sodium Hydroxide Molarity on the Compressive and Splitting Tensile Strength of Ferronickel Slag-Based Alkali Activated Mortar," 2021. doi: https://doi.org/10.14710/mkts.v27i2.32706.
7. A. Antoni, F. Hartono, S. Tanuwijaya, K. Wijaya, A. Vianthi, and D. Hardjito, "Comprehensive Investigation on the Potential of Fly Ash from New Source as Construction Material," *Civil Engineering Dimension*, vol. 23, no. 2, pp. 78–90, Oct. 2021, doi: 10.9744/ced.23.2.78-90.
8. S. R. Hunchate, S. Chandupalle, Vaishali. G. Ghorpode, and V. Reddy, "Mix Design of High Performance Concrete Using Silica Fume and Superplasticizer ," *Int J Innov Res Sci Eng Technol*, vol. 3, no. 3, Mar. 2014.
9. G. A. Rao, "Role of water–binder ratio on the strength development in mortars incorporated with silica fume," *Cem Concr Res*, vol. 31, no. 3, pp. 443–447, Mar. 2001, doi: 10.1016/S0008-8846(00)00500-7.
10. V. Monov, B. Sokolov, and S. Stoenchev, "Grinding in Ball Mills: Modeling and Process Control," *CYBERNETICS AND INFORMATION TECHNOLOGIES*, vol. 12, no. 2, pp. 51–68, 2012.
11. S. A. A. M. Fennis and J. C. Walraven, "Using particle packing technology for sustainable concrete mixture design," *HERON*, vol. 57, no. 2, pp. 73–101, 2012.
12. A. K. H. Kwan and C. F. Mora, "Effects of various shape parameters on packing of aggregate particles," *Magazine of Concrete Research*, vol. 53, no. 2, pp. 91–100, Apr. 2001, doi: 10.1680/macr.2001.53.2.91.
13. A. Kuncoro, D. R. Paramitha, L. Y. Meok, A. Antoni, and D. Hardjito, "ANALISIS PENGARUH VARIASI PENGGUNAAN BAHAN ADITIF TAMBAHAN SUPERPLASTICIZER TERHADAP PROPERTI PASTA KOMBINASI SEMEN-FLY ASH," *Rekayasa Jurnal Teknik Sipil Universitas Madura*, vol. 8, no. 1, pp. 29–35, Jun. 2023.

14. M. A. Bajaber and I. Y. Hakeem, "UHPC evolution, development, and utilization in construction: a review," *Journal of Materials Research and Technology*, vol. 10, pp. 1058–1074, Jan. 2021, doi: 10.1016/j.jmrt.2020.12.051.
15. ASTM C618-22, "Standard Specification for Coal Fly Ash and Raw or Calcined Natural Pozzolan for Use in Concrete," 2022.
16. X. Fu, Q. Li, J. Zhai, G. Sheng, and F. Li, "The physical–chemical characterization of mechanically-treated CFBC fly ash," *Cem Concr Compos*, vol. 30, no. 3, pp. 220–226, Mar. 2008, doi: 10.1016/j.cemconcomp.2007.08.006.
17. O. Ofuyatan, A. Olowofoyeku, J. Oluwafemi, and J. Ighalo, "Predicting the Compressive Strength of Concrete By Ultrasonic Pulse Velocity," *IOP Conf Ser Mater Sci Eng*, vol. 1036, no. 1, p. 012053, Mar. 2021, doi: 10.1088/1757-899X/1036/1/012053.

# GCEE

ORIGINALITY REPORT

| 7% | 6% | 5% | 1% |
|---|---|---|---|
| SIMILARITY INDEX | INTERNET SOURCES | PUBLICATIONS | STUDENT PAPERS |

PRIMARY SOURCES

| | | |
|---|---|---|
| 1 | repository.petra.ac.id<br>Internet Source | 2% |
| 2 | Zhaoheng Guo, Pengkun Hou, Zhenhai Xu, Jianming Gao, Yasong Zhao. "Sulfate attack resistance of tricalcium silicate modified with nano-silica and supplementary cementitious materials", Construction and Building Materials, 2022<br>Publication | 1% |
| 3 | Submitted to Asian Institute of Technology<br>Student Paper | <1% |
| 4 | uia.brage.unit.no<br>Internet Source | <1% |
| 5 | Leidy T. Vargas-Ibáñez, Christian O. Díaz-Ovalle, José J. Cano-Gómez, Gerardo A. Flores-Escamilla. "Theoretical analysis of the spray characteristics of ternary blends of diesel, biodiesel, and long-chain alcohols inside a combustion chamber", Fuel, 2023<br>Publication | <1% |

| | | |
|---|---|---|
| 6 | www.researchgate.net<br>Internet Source | <1% |
| 7 | S. A. M. Binhowimal, L. Hanzic, J. C. M. Ho. "Filler to improve concurrent flowability and segregation performance of concrete", Australian Journal of Structural Engineering, 2017<br>Publication | <1% |
| 8 | journals.pan.pl<br>Internet Source | <1% |
| 9 | kemahasiswaan.uhamka.ac.id<br>Internet Source | <1% |
| 10 | www.scielo.br<br>Internet Source | <1% |
| 11 | Jiachen Guo, Tak-Ming Chan, Yuhong Wang. "Experimental investigation on the structural performance of the high-strength ring strengthened dowel connection under monotonic load", Engineering Structures, 2023<br>Publication | <1% |
| 12 | Mehran Aziminezhad, Mahdi Mahdikhani, Mohammad Mahdi Memarpour. "RSM-based modeling and optimization of self-consolidating mortar to predict acceptable | <1% |

ranges of rheological properties",
Construction and Building Materials, 2018
Publication

| | | |
|---|---|---|
| 13 | downloads.hindawi.com<br>Internet Source | <1 % |
| 14 | mdpi-res.com<br>Internet Source | <1 % |
| 15 | oda.oslomet.no<br>Internet Source | <1 % |
| 16 | repository.its.ac.id<br>Internet Source | <1 % |
| 17 | scholarsmine.mst.edu<br>Internet Source | <1 % |
| 18 | manufakturindo.com<br>Internet Source | <1 % |

| | | | |
|---|---|---|---|
| Exclude quotes | On | Exclude matches | < 5 words |
| Exclude bibliography | On | | |